Investigation of Fast, Secure and Reliable Network Restoration after Blackouts

Elmira Torabi Makhsos [1],*, Yi Guo [1], Wolfgang Gawlik [1],*, Benjamin Cox [1], Philipp Hinkel [2], Marian Zugck [2], Wolfram Wellßow [2], Robert Schmaranz [3], Ewald Traxler [4] and Leopold Fiedler [4]

[1] Institute of Energy Systems and Electrical Drives, Technische Universität Wien, 1040 Vienna, Austria; guo@ea.tuwien.ac.at (Y.G.); cox@ea.tuwien.ac.at (B.C.)

[2] Division of Energy Systems and Energy Management, Technische Universität Kaiserslautern, 67663 Kaiserslautern, Germany; hinkel@eit.uni-kl.de (P.H.); zugck@eit.uni-kl.de (M.Z.); wellssow@eit.uni-kl.de (W.W.)

[3] KNG-Kärnten Netz GmbH, 9020 Klagenfurt am Wörthersee, Austria; robert.schmaranz@kaerrnetz.at

[4] Netz Oberösterreich GmbH, 4030 Linz, Austria; ewald.traxler@netzgmbh.at (E.T.); leopold.fiedler@netzgmbh.at (L.F.)

* Correspondence: torabi@ea.tuwien.ac.at (E.T.M.); gawlik@ea.tuwien.ac.at (W.G.)

check for updates

Abstract: Integrating distributed generation into power grids creates various technical challenges for network operation. Volatility of renewable energy resources may increase the probability of blackouts. In order to restore networks fast, securely and reliably after blackouts, within the research project RestoreGrid4RES's network restoration strategies, the related issues caused by distributed generation are investigated and novel methods to face those challenges are developed. This paper focuses on (i) algorithms to identify possible restoration paths, (ii) key performance indicators for the assessment of grid restoration options and (iii) an evaluation of the results for network restoration strategies.

Keywords: power system restoration; distributed generation; optimization algorithm; key performance indicator

1. Introduction

During system restoration, high shares of distributed generation (DG) which is often in the form of renewable energy sources (RES) with automatic synchronization characteristics may lead to system instability and an increased risk of a second blackout [1]. The integration of DG in the distribution network is one of the main focuses during system restoration [2] and the frequency and voltage stabilities of this type of network have been investigated in the following literature [3,4]. Nevertheless, presently, there is not a lot of experience concerning the operation of DG during a system restoration. The problem of large-scale DG sources during restoration is rarely investigated.

In addition, the peak value of loads after an interruption can be significantly higher than that at normal operation, which causes additional challenges. This is known as cold load pick-up (CLPU) [5–8]. For a typical restoration process, the important issues are summarized in the literature [9–11]. Hence, the aim of the project RestoreGrid4RES is to evaluate current power system restoration (PSR) concepts and to develop new advanced, fast and secure PSR strategies considering a high penetration of DG. This work was initiated by the presented studies in [12–14].

As a first step, a review of the legal framework, technical requirements and existing network restoration strategies, and an analysis of the impact of the volatility of DG have been carried out [15]. Then, based on the review and the experience of Austrian distribution system operators (DSO), new restoration strategies are developed [12].

Responsibility for the restoration lies with the transmission system operators (TSO), however, many DSO have the capability to restore their distribution system with black start units (BSU), too. Based on the developed PSR strategy matrix, this paper only considers restoration according to the build-up strategy [12].

Then, an automated system restoration algorithm was carried out to calculate PSR paths. This algorithm combines the Monte Carlo tree search with depth-first search and breadth-first search including a load flow calculation and dynamic analysis. In order to have access to all generated path data and system properties during the restoration, the algorithm is connected to an external database. Besides, to accelerate path generation, this algorithm is executed in parallel on supercomputers.

To evaluate and compare the PSR paths, key performance indicators (KPI) are used. The restoration process is simulated on a real distribution network. The aims of this automated restoration concept are as follows:

- To generate as many paths as possible, considering steady and dynamic system characteristics;
- To preserve all calculated data during the restoration process;
- To accelerate the calculation;
- To find different types of restoration strategies (focus for future work).

The paper is organized as follows: Section 2 illustrates the off-line automatic system computation that is implemented for network restoration. Section 3 considers the system dynamic characteristics. Section 4 analyzes the proposed automated depth-first search (DFS) and breadth-first search (BFS) algorithm and the extended parallelization. Section 5 elucidates the global and individual KPI. Section 6 gives a description of the network model and simulation environment as well as the evaluation of the results to develop PSR strategies for future work.

2. Automated System Restoration Computation

The restoration process of the entire electrical grid is represented as a large and high-dimensional decision tree-like directed acyclic graph, consisting of edges and nodes. Searching algorithms for graphs is necessary to find connected nodes representing intermediate grid states and to traverse the entire graph. The edges of the graph are operator actions and nodes are grid states following these actions [13]. In order to speed up the computation time, the indicated algorithm is extended to be executed in parallel on a high number of processors. To achieve this goal, the developed algorithm is run on the Vienna Scientific Cluster (VSC-3)—the most powerful Austrian supercomputer at the time (http://vsc.ac.at/). Furthermore, an external MySQL database is necessary to store all calculated nodes and to optimize search strategies and the distributed computing. Furthermore, to shorten the communication time, the indicated algorithms are extended to save the calculated children nodes on a MySQL database located in VSC.

The flow chart in Figure 1 represents an automated restoration algorithm, including both the load flow calculation and evaluation of the system's dynamic behavior. The MATLAB code executes one possible switching action after the other and calculates each new network state.

In the first step of the automated restoration algorithm, the network to be restored is initialized with pre-defined system parameters, e.g., amount and location of elements, rated power of generators, impedance of power lines, terminals of transformers, etc. Afterwards, the configuration of possible starting grids is loaded into the simulation. The starting grid may consist of a single BSU in operation or any other configuration with already re-connected load, generators or power lines. The starting grid in this paper consists of the black start-capable hydro power plants [5], which are located in the distribution network of Carinthia.

Furthermore, in this step, the security limits including boundary conditions and influencing parameters, such as the start-up frequency, voltage, maximum load and generation, are loaded. To check whether the starting grids are feasible, a load flow calculation is carried out. If the system's

physical values after the load flow calculation are within the limits, all individual possible actions for this system state will be performed.
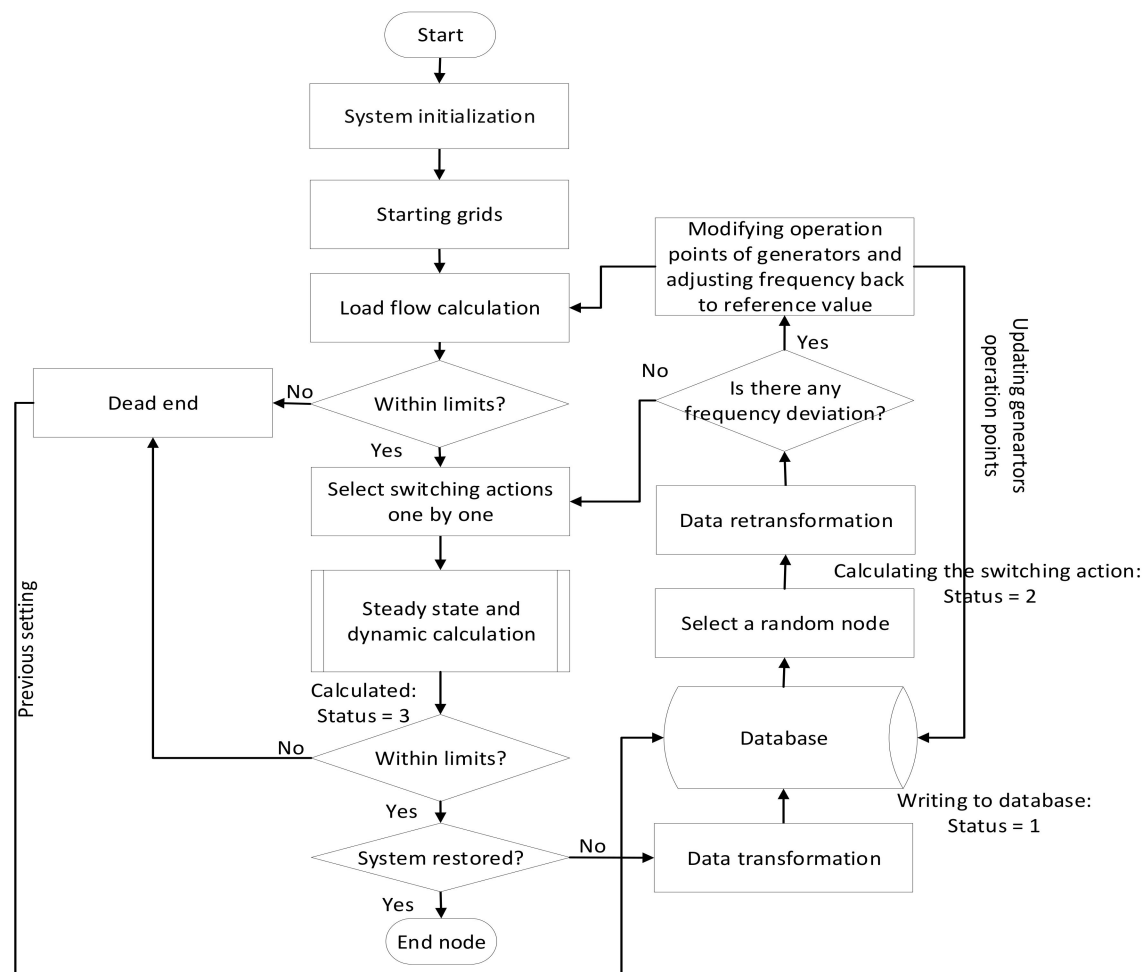
Figure 1. Flow chart—overview of algorithms.

The system's physical values that are observed to be within limits are as follows. A dynamic calculation is carried out independently from the load flow calculation:

- Maximum and minimum dynamic frequency;
- Static frequency;
- Maximum and minimum voltage at substations;
- Loading of lines and transformers;
- Generators' operation points.

Each individual resulting state of the network is generated following the individual possible action and steady state and dynamic calculations are performed. This includes load flow calculation, system steady state and dynamic frequency deviation and cold load pick-up, to investigate the possible new states of the network.

Figure 1 shows this approach. For simplicity, the inner loop handling all possible switching actions one by one is not presented in detail. Available switching actions that are applied in the simulation include the following:

- Energizing power lines;
- Energizing transformers;

- Connecting loads;
- Synchronizing generators.

If the system's physical values—as indicated before—after an initial load flow calculation are within the security limits, the individual resulting network and its values ("node") are stored in a MySQL database with a status of "1" (meaning "new node") through Python modules. The next node in the database is selected among those existing "status 1" nodes based on a strategy described in Section 4. The data of the selected node will be retransformed and prepared for the next calculation in MATLAB. Once the node is chosen, the status of this node in the database is changed to "2" (meaning "currently being explored"). This avoids multiple selection during the calculation. After the load flow calculation and the creation of the multitude of resulting nodes, the status of the node is updated to "3" (meaning "explored"). The Python modules are implemented to transform, retransform and update the data as well as communicate between MATLAB and the MySQL database. The generated data structure in MATLAB is complex and incompatible with the MySQL database. The Python modules transform the generated MATLAB data into a table format to save the system properties in the MySQL database. Afterwards, a random node is selected from the database and the data structure is retransformed for further calculation in MATLAB.

Besides the strategies in Section 4, which are based on the Monte Carlo tree search [16], it would be possible to set priorities to re-connect loads. However, the priorities can limit the variety of random choices and reduce the number of generated possible PSR paths. The focus of this paper is on the randomly generated PSR paths, therefore, priorities are not further discussed.

The steady state frequency deviation occurring during the restoration after the connection of loads or generators is adjusted through modifying the operation points of the activated generators within their limits before a set of new switching actions is explored, mimicking automated or manual frequency restoration.

3. System Dynamic Characteristics

The system static characteristics were discussed in a work published earlier [13]. In order to improve the trustworthiness of the performed simulations, short-term (in the range of seconds) and medium-term (in the range of minutes) system dynamic characteristics, such as frequency response, CLPU and the automatic or manual adaption of operation points of generators, are considered [17,18]. However, to limit the complexity of the approach, long-term developments, e.g., of loads and generation throughout several hours, are omitted.

To ensure a secure restoration, the network is re-energized step by step. The algorithm depicted in Figure 2 calculates what part of a lumped load in each step can be re-connected. If the connection of the entire load exceeds the security constraints, only a chunk of the load with a predefined granularity (e.g., in 10% steps) is connected to maintain the previously exceeded parameter within the allowable range.

This approach considers that the lumped substation load in the model represents loads distributed to several feeders that can be re-connected individually. The algorithm with adapted steps of a predefined percentage (e.g., 10%) has been chosen to represent that several combinations may be possible, but can be adapted or even omitted for a worst-case scenario with less flexibility [19].

As it is depicted in Figure 1, if after the load connection the security limits are violated, this node is identified and saved as a dead end node. The system will be reverted to the previous state and another unexplored node will be selected.

Splitting a lumped load into smaller portions is beneficial for the restoration process, as the dynamical CLPU behavior of the loads to be re-connected needs to be considered both in the calculations and the real restoration process.
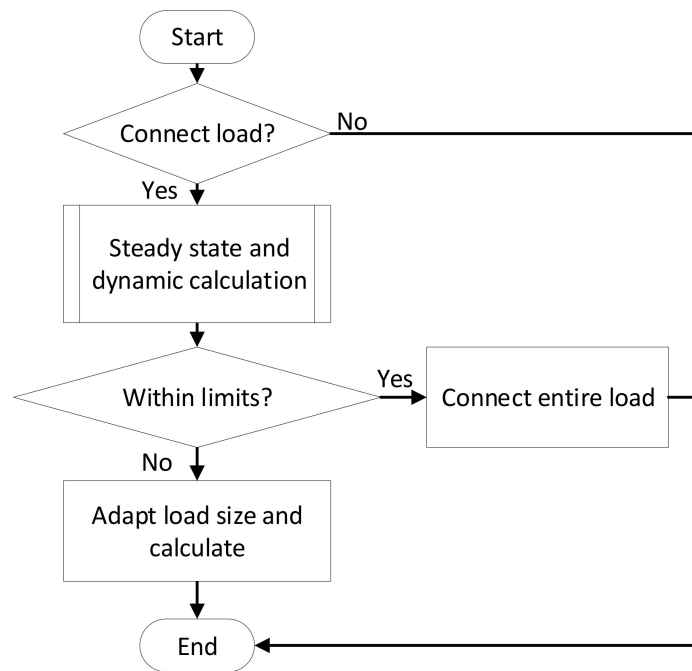
Figure 2. Load connection in adapted chunks.

The CLPU behavior considered in the simulations and dynamic frequency characteristic of a load re-connection are depicted in Figure 3 with the following equations, where P_{state} is the steady state load:

$$P(t) = P_{state} * K_{CLPU}(t), \tag{1}$$

$$K_{CLPU}(t) = \begin{cases} 1 & t < t_B \\ 0 & t_B \leq t < t_R \\ K_{MAX} & t_R \leq t < t_H \\ (K_{MAX} - 1) * e^{-(t-t_H)/T_{CLPU}} + 1 & t < t_H \end{cases}, \tag{2}$$

In Equation (2), t_B represents the time when the load is disconnected, and t_R is the re-connection time for a cold load. CLPU factor K_{CLPU} is at maximum value K_{MAX} during the time interval between t_R and the hold time t_H. Afterwards, the time constant T_{CLPU} of the active power exponential decay starts from t_H. As typical values found in previous studies, the factors $K_{CLPU} = 2.5$ and $T_{CLPU} = 600$ s have been chosen [8,20]. For the re-connection process shown in Figure 3, the load is connected at $t_R = 10$ s after being disconnected at $t_B \ll 0$ s. The hold time t_H. is set to 50 s. The dashed line is the CLPU behavior and the solid line shows the simulated dynamic frequency response following a load re-connection. The frequency response after load re-connection is most critical in the first phase of the system restoration, as only little inertia is in the system and the system frequency is more likely to collapse again. The highest frequency deviations $\Delta f_{max,dyn}$ and $\Delta f_{min,dyn}$ depend on the size of the connected load and the system dynamic characteristics. Thus, the load is connected in the indicated algorithm to ensure a stable restoration.

The generator units are assumed to ramp up to their operating point rather slowly after being re-synchronized, which leads to much less critical system dynamic behavior than that caused by load re-connection. Therefore, the dynamic frequency response of the system is only investigated for load re-connections. However, the steady state frequency deviation is considered for both cases. In order to avoid overloading of branches and voltage band violations after the load connection, the active power demand of the load is distributed over all active generators in the system participating in load frequency control according to their droop settings [21]. To recover the system frequency to its reference value f_0, which may be chosen to be different from 50 Hz, e.g., slightly higher, active power set points

of generators are adapted accordingly after the load connection. For example, the reference frequency has been chosen as 50.7 Hz in the DSO network to be restored as described in Section 6.1. This provides a wider range for both negative (usually higher) and positive dynamic frequency deviations during the load re-connection.
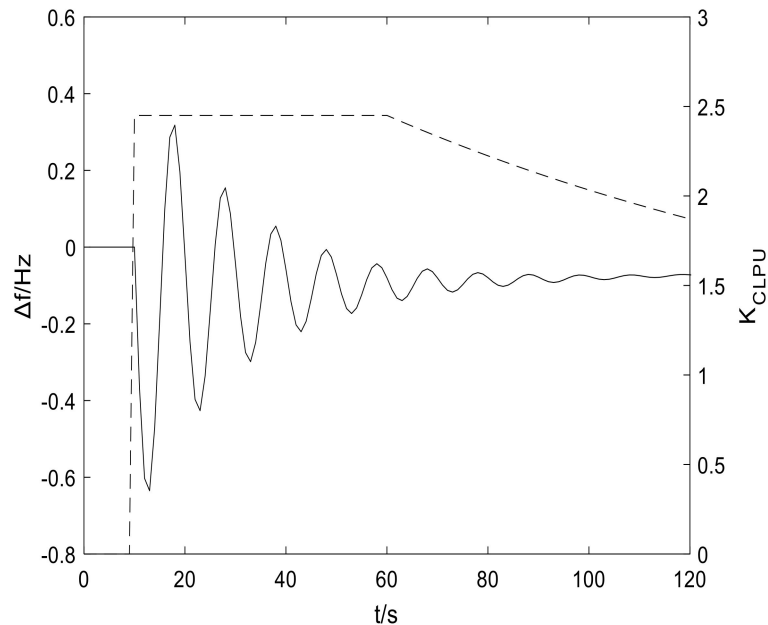

Figure 3. Frequency response of the system after a load connection.

4. Path Identification Algorithms

Network restoration processes are modeled as a very large tree-like directed acyclic graph [16]. The graph presented in Figure 4 demonstrates the network restoration tree. The root of the tree is the starting point $\varrho \in \{R_{0-1}, R_{0-2}, \ldots, R_{0-NR}\}$, where zero defines the root level and N_R defines the number of starting points in the network. Each starting point may have a different configuration depending on the chosen restoration strategy. Each node is designated as S_{l-j}, where l is the so-called level, i.e., the number of switching actions, which have been performed to reach it, and j an index for the nodes of each level, going from 1 to N_j. In Figure 4, each node in the network except the root nodes originates from its parent node, which in turn has a set of the children nodes. The states in the tree are connected by edges that are representing switching actions. The incoming edge connects a specific node to its parent node and outgoing edges connect a specific node to its children nodes [22].

Obviously, with increasing j, the number of nodes in the level N_j can be expected to increase significantly, at least close to the root of the tree. The Monte Carlo approach combined with a DFS and BFS are two mechanisms used to identify nodes and edges in the graph. They are described in this section and make use of the level of the nodes.
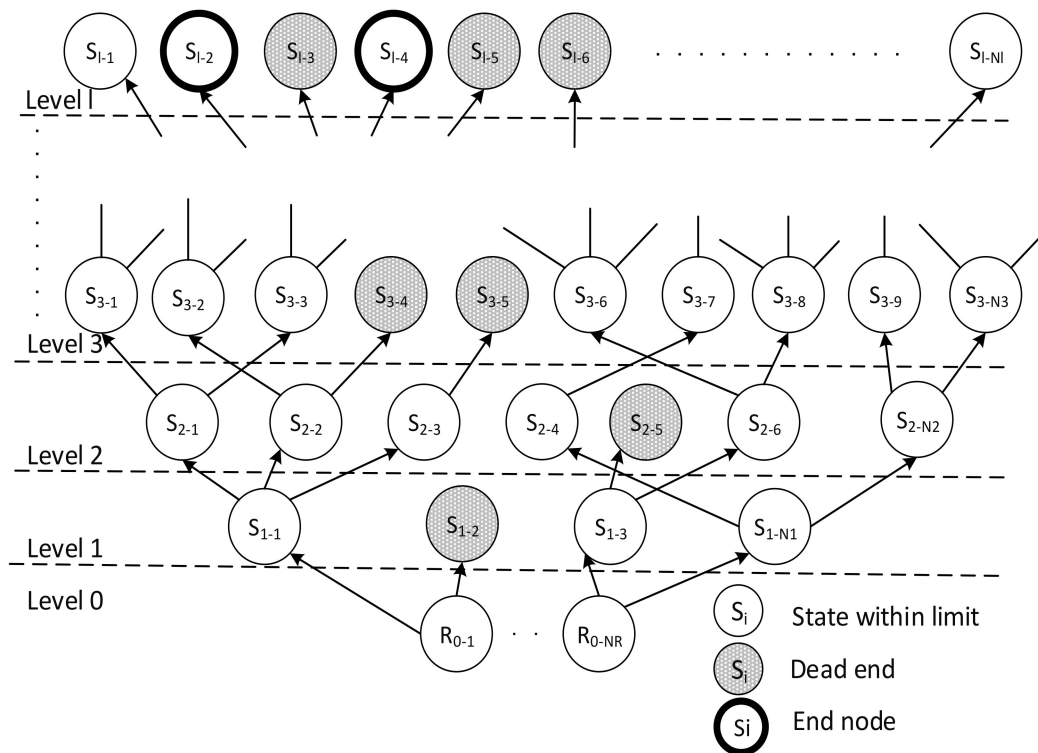
Figure 4. General representation of the network restoration tree.

4.1. Depth-First Search and Parallel Depth-First Search

DFS illustrates the search algorithm, which means that each processor following this approach starts at the lowest available level and calculates one unexplored node from that level. Then, it continues to select an unexplored node of the next level (last-in, first-out). This method quickly leads away from the starting point. The path can reach a higher level much faster in comparison with BFS, explained below.

For example, R_{0-1}-S_{1-1}-S_{2-2}-S_{3-2} ... -S_{l-2} depicts a possible path as shown in Figure 4. However, if a suitable restoration path or only dead ends are found, it would only be trying alternative approaches from the same level on. Therefore, the nodes to be calculated in the tree are chosen randomly out of the unexplored nodes of the next level except when the DFS reaches an end node or no unexplored nodes of the next level are available. In the first case, the DFS approach steps back to an unexplored node of the lowest available level. This is to avoid generating only paths, which are identical on all initial actions but the very last ones. In the second case, the processor selects an unexplored node of the same level, or, if no unexplored nodes are available on that level, successively from the next level below.

To speed up creating possible paths, the MATLAB code is parallelized on multiple processors (parallel DFS strategy) on VSC [23]. Each processor selects one unexplored node of its next level available and starts calculating all children nodes.

Figure 5 shows this for three processors. If one processor has finished its task, it can select an unexplored node created by another processor. For example, the processor 3 can choose the node S_{2-3}, whose parent node is S_{1-1}, created by processor 1 and continue the calculation from this node. As more than one processor is used to generate the paths in the same database, the number of paths reaching high levels is increased during the same time in comparison with using one MATLAB script with DFS.
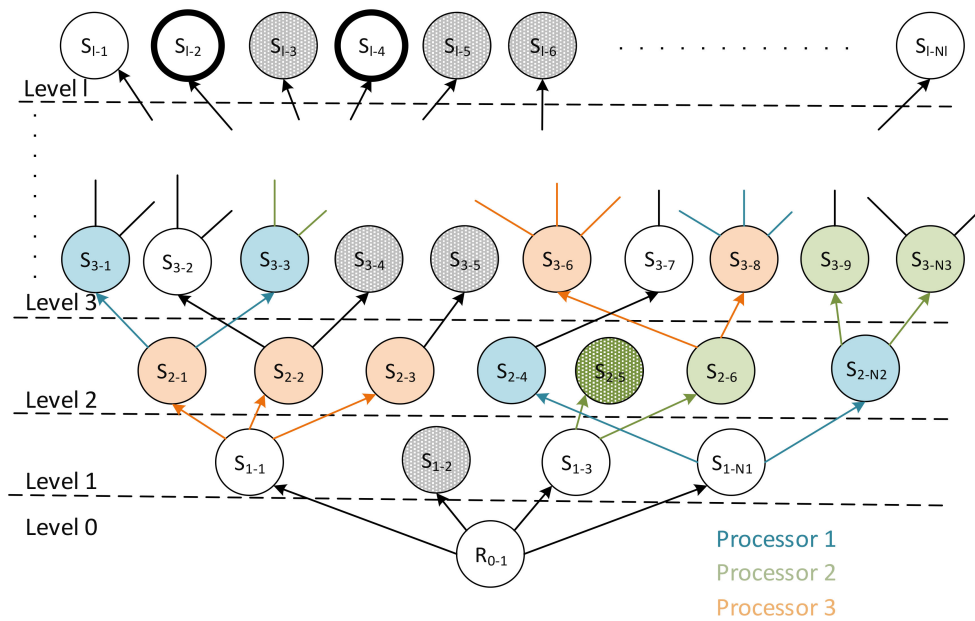
Figure 5. Parallel depth-first search strategy.

4.2. Own Depth-First Search and Parallel Own Depth-First Search

In order to be able to compare different paths of the re-energizing processes which are different right from their starting point, the following search algorithm is developed.

Own DFS (oDFS) is such an approach to identify several possible paths which are different in their early actions. Similar to the parallel DFS strategy, the MATLAB code runs on several processors in parallel. The main difference from parallel DFS is that parallel oDFS only allows randomly selecting nodes among the next level nodes generated by the same processor. Hence, paths are built up independently from each other.

Figure 6 shows the parallel oDFS strategy. As can be seen, one processor starts the calculation first and after a certain delay, other processors start to select available unexplored nodes from the lowest level. Therefore, paths can be created in parallel based on the initial nodes selected by the processors.
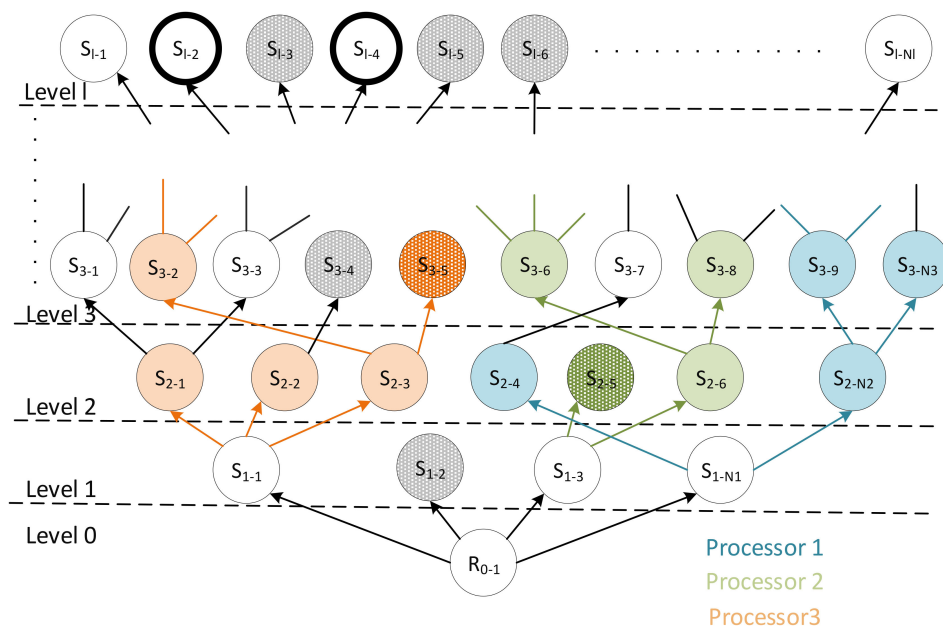

Figure 6. Parallel own depth-first search strategy.

4.3. Breadth-First Search

BFS is comparable to storing the discovered nodes in a queue (first-in, first-out). This means that exploring the graph is done from an unexplored node of the lowest level (i.e., the oldest node in the queue) and radiates out slowly from the starting point(s). In the first step, the MATLAB code calculates, and the Python code stores all possible nodes within level 1, and later up to level *l*. For example, in Figure 4, the calculating begins with $R_{0\text{-}1}$. By switching actions, starting point $R_{0\text{-}1}$ reaches its children nodes $S_{1\text{-}1}$ and $S_{1\text{-}2}$. Level 1 nodes are the children nodes from starting point $R_{0\text{-}i}$ and have the parent-id of their start node. After all level 1 nodes are found and calculated, it starts the same search and calculation procedure with the next level 2 and continues up to the highest level, *l*, until the last switching action to the children node $S_{l\text{-}Nl}$ is carried out.

The parallel BFS (pBFS) strategy is used to speed up the path's calculation. For the execution of the pBFS strategy, the same MATLAB and Python codes will be running on several processors and each processor can access the generated nodes from the other processors [24]. All calculated nodes will be stored in the MySQL database.

Worth to mention, pBFS is found to be suitable to create a large variety of starting points for oDFS.

4.4. Random Search

For a random search, the next node for a processor to be explored is selected randomly out of all unexplored nodes, irrespective of its level. After choosing a random node, the calculation is performed as in the other algorithms mentioned above and all its possible children nodes are stored in the database. Thus, the graph can be built up completely randomly. However, no quick results in terms of restoration after a long calculation time may be found.

5. Key Performance Indicators

Global and individual KPI are defined in the project to check whether the network restoration paths are efficient, reliable and secure or not. Part of the global and individual KPI evaluated in this paper are presented in this section.

5.1. Global Key Performance Indictors

Global KPI consider the total restoration process, or at least a significant period during the restoration process. To check how long the whole restoration process takes, time to full system restoration, the number of switching actions required and energy that is provided during the restoration are investigated.

Restoration time T_{FSR} is the time elapsed from the beginning of the system restoration process until the system is restored, e.g., 50% of total load being supplied can be defined as a restored system. The number of switching actions represents how much time is required for the different actions until the system is restored, e.g., voltage forwarding, connection of loads, synchronization and re-connection of generators and changing set points. With the power provided by the system, $P_{system}(t)$, and assuming that the system restoration process starts at $t = 0$, the energy provided during the restoration process E_{FSR} is

$$E_{FSR} = \int_0^{T_{FSR}} P_{system}(t)dt, \tag{3}$$

A higher value of E_{FSR} is featured by those PSR paths where the loads mostly are connected in larger chunks and the power system is re-energized within a lower restoration duration. This value can be divided by the specific time required for system restoration.

$$P_{FSR} = \frac{\int_0^{T_{FSR}} P_{system}(t)dt}{T_{FSR}}, \tag{4}$$

Thus, this KPI becomes the average power served during the system restoration. Finally, the rate of increase in the power demand to be handled by the system, which indicates the speed of the restoration, can be calculated. Over the restoration time T_{FSR}, the rate of power increase is

$$\dot{P}_{FSR} = \frac{\int_0^{T_{FSR}} P_{system}(t)dt}{T_{FSR}^2}, \tag{5}$$

Considering the speed of the PSR paths, the paths with higher values of $\dot{P}_{FSR}$ might have priority for grid operators.

With $f(t)$ being the actual system frequency and f_0 the reference frequency, the highest frequency deviation Δf_{max} is

$$\Delta f_{max} = \max_t \left| f(t) - f_0 \right|, \tag{6}$$

As the single maximum value defined above may be caused by a singular situation during the system restoration process, it might be reasonable to consider an integral of this value over the restoration time. However, this would require normalizing the result with the total time to system restoration, as otherwise, restoration paths requiring a longer time might automatically be at a disadvantage in this criterion. The integral of frequency deviations over the entire restoration time Δf_{int} t is calculated as

$$\Delta f_{int} = \frac{\int_0^{T_{FSR}} \left| f(t) - f_0 \right|}{T_{FSR}}, \tag{7}$$

A higher value of frequency deviation is characterizing those PSR paths where the system load ability is more often used during the whole restoration process. Nevertheless, the frequency deviation effect is more critical at the beginning of the restoration. If a large load is connected as a whole, it can cause a dynamic instability in the network.

With $v_i(t)$ being the voltage of each node i over the system restoration time in p.u., the highest voltage deviation is

$$\Delta v_{max} = \max_{i,t} \left| v_i(t) - 1 \right|, \tag{8}$$

Likewise, the integral of voltage deviation Δv_{int} is defined as

$$\Delta v_{int} = \frac{\int_0^{T_{FSR}} \left| v(t) - 1 \right|}{T_{FSR}}, \tag{9}$$

The voltage deviation is visible and critical at the later stage of restoration. The minimum voltage value is close to the security limit, which means that in the later steps, reactive power management is necessary.

The KPI are calculated and compared for restoration paths with different numbers of action steps and durations. Therefore, the time series of system values used for the calculation of KPI needs to be amended in a suitable manner (e.g., extended to the duration of the longest path in the selection) to allow a valid comparison.

5.2. Individual Key Performance Indicators

Individual KPI are valid only for a specific state occurring during the system restoration. Generally, any individual KPI may be made global by integrating or averaging it over the system restoration time. However, it has to be checked whether the result should then be normalized, as this value might differ significantly.

The average load step during system restoration $\overline{\Delta P}_{system}$ is defined as the re-energized load demand in the last step $P_{system,\,end}$ divided by the number of steps $N_{connected\_load}$ where loads are reconnected during the PSR:

$$\overline{\Delta P}_{system} = \frac{P_{system,\,end}}{N_{connected\_load}},\tag{10}$$

The objective of this KPI is to give an overview of the load step ability in the system during the whole restoration process. By considering the high value of $\overline{\Delta P}_{system}$, corresponding restoration paths finish earlier and require less restoration time. Additionally, the system load step ability is defined by the maximum load step $\Delta P_{\max\_load}[n]$ that the system can support during transient conditions and in steady state without reaching critical frequency limits. The average use of the load step ability during system restoration $\overline{\Delta P_{load\_step\_ability}[n]}$ is the actual change of power $\Delta P_{system,load}[n]$ provided by the system when a load is re-connected and divided by the maximum load step. It is the average value, which shows how much of the load step ability in the system has been used at each step. Variable n indicates the level, where the load is re-energized.

$$\overline{\Delta P_{load\_step\_ability}[n]} = \sum_{n=0}^{N_l} \frac{\Delta P_{system,load}[n] / \Delta P_{\max\_load}[n]}{N_n},\tag{11}$$

A high value of both KPI indicates a faster restoration process. Combinations of these values and the maximum power reserve can be used as individual KPI, too.

6. Network Model and Simulation Results

### 6.1. 110 kV Carinthia Distribution Network Model

The simulation results of PSR are based on a real distribution grid with data provided by the Austrian DSO KNG-Kärnten Netz GmbH (Carinthia Network). The length of the 110 kV network is 850 km with 100% overhead power lines and the length of the 20 kV network is more than 5800 km with 51% of overhead power lines. The network contains 215 branches (93 power lines and 122 transformers) within the interconnected 110 kV and 20 kV system and 158 busses. The model includes 37 hydro generators. The restoration starts with the black start- and island-capable hydro power plants in the Carinthia network.

6.2. Evaluation of Simulation Results

In order to illustrate the evaluation of restoration strategies and identification of the best strategy, during the RestoreGrid4RES project, a significantly larger number of restoration paths with 50% of re-energized load demand are compared. The proposed algorithms are performed on multiple processors on the Vienna Scientific Cluster and implemented in MATLAB R2016b. To perform the load flow calculations, MATPOWER package 5.1 is applied. Based on the developed PSR strategy matrix, a combination of the bottom-up and build-up strategy is applied [12].

PSR begins with the black start-capable units in the Carinthia network at the determined reference frequency of 50.7 Hz. A combination of parallel BFS and parallel oDFS is applied. All children nodes of initial states are calculated through parallel BFS by executing MATLAB scripts on parallel processors. Afterwards, all children nodes of nodes in level 1 are calculated up to level 3. The generated children nodes from this level are defined as initial states for parallel oDFS [14].

Figure 7 depicts the process of load re-energization regarding the required restoration time in each level for the 331 generated PSR paths (Tables S1–S331). The red solid line is the manually generated reference path—Path-No. 331 according to the PSR concept of the Carinthia network power supply company. The dashed line shows the PSR path with the shortest required time for 50% of the re-energized load demand, which is determined as Path-No. 140 and the dotted line depicts the Path-No. 123 with the longest required supply time.
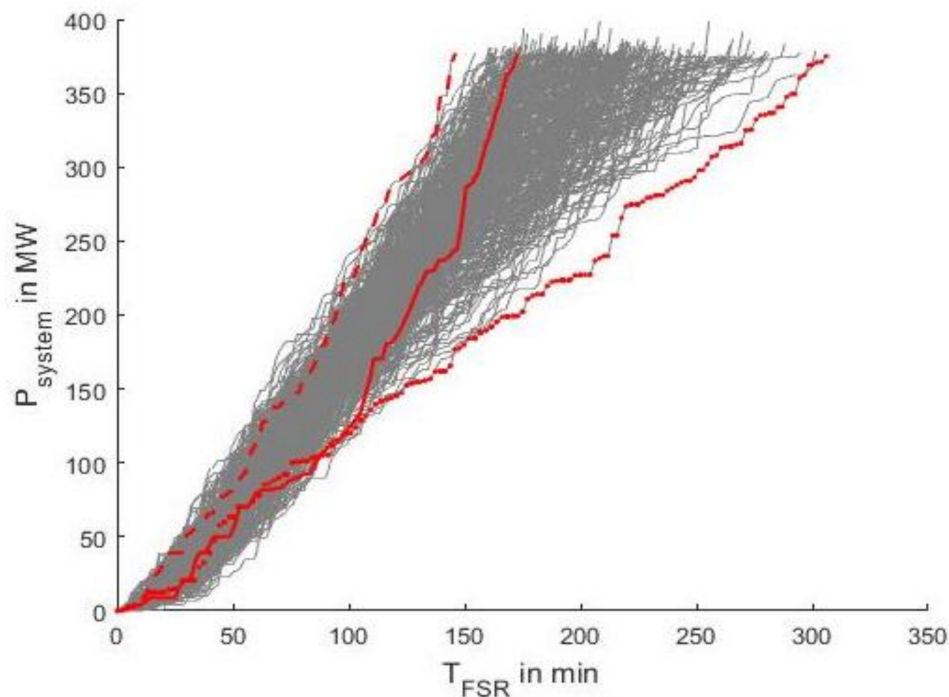
Figure 7. Restoration process of grid for 331 PSR paths: Red solid line is the manually generated standard path—Path-No. 331, dashed line is the fastest Path-No. 140, dotted line is the slowest Path-No. 123 (Tables S1–S331).

The total load demand for the study case is 750 MW which means that the system is assumed to be successfully restored if more than 375 MW load in the network is supplied. Depending on the load size that is chosen for the last step of switching action to the successful restoration, the load supply at the end of one path can be larger than 375 MW.

For example, in Path-No. 331, the maximum load step that can be supported during the last switching action is approximately 40.05 MW. As long as the load step size is smaller than 40.05 MW, it can be switched on without reaching system critical limits. Therefore, the re-energized load demand in the last level $P_{system}(172.83 \text{ min})$ reaches 376.95 MW by carrying out a 9.60 MW load step from the second last status $P_{system}(170.83 \text{ min})$ being 367.35MW. In Path-No. 140, the re-energized load demand in the last level $P_{system}(146.16 \text{ min})$ is 376.97 MW and in Path-No. 123, $P_{system}(306.00 \text{ min})$ is 375.05 MW.

As reported in [14], the required time for a load re-connection is assumed to be 120 s because of the system dynamic frequency response after a cold load pick-up. The idle generators are re-energized and slowly ramped up to their operating point to get ready for re-synchronization. The time for generator re-synchronization is thus set to 90 s. Furthermore, the active power of the load demand is distributed over all activated generators. The time that is assumed for re-energizing power lines or transformers by network operators is 10 s.

In those generated paths where more power lines or transformers are connected or in those paths where loads are connected in smaller steps, the restoration time is usually higher. More switching actions are needed until required loads are connected, leading to a longer restoration time, and thus higher delivered energy. Table 1 shows the comparison of normalized provided energy, average supplied power and the rate of increase of supplied power demand during the system restoration.

Table 1. Evaluation of the restoration process.

| Path-No.	E_{FSR}/MWh [1]	P_{FSR}/MW	$\dot{P}_{FSR}$/MW/h	T_{FSR}/min
331 (reference)	247.85	101.16	41.29	172.83
140 (fastest)	387.35	158.10	64.53	146.16
123 (slowest)	212.50	86.73	35.40	306.00

[1] Values calculated at $T_{FSR} = 146$ min.

In order to compare restoration paths using KPIs described in the previous chapter, the same time basis is required. The following results for all paths are calculated at $T_{FSR} = 146$ min. Regarding the provided energy and average power served and power gradient during the system restoration, Path-No. 140 has the highest value.

The pie charts in Figure 8 compare the share of reconnected elements at the end of the rebuilding process for the selected paths (Table S332). In Path-No. 140, the number of reconnected loads is lower than in other paths, which means that loads are connected in larger steps. Besides, the low amount of re-synchronized generators leads to higher frequency deviations. However, the share of transformer and the power line energizations is higher. Path-No. 331 illustrates a dynamically stably restored system with a high contribution of re-synchronized generators and re-connected loads. Path-No. 123 represents the path with the greatest number of switching actions, leading to a longer restoration time. In Figure 8, the number of activated generators excludes the number of initial BSU.
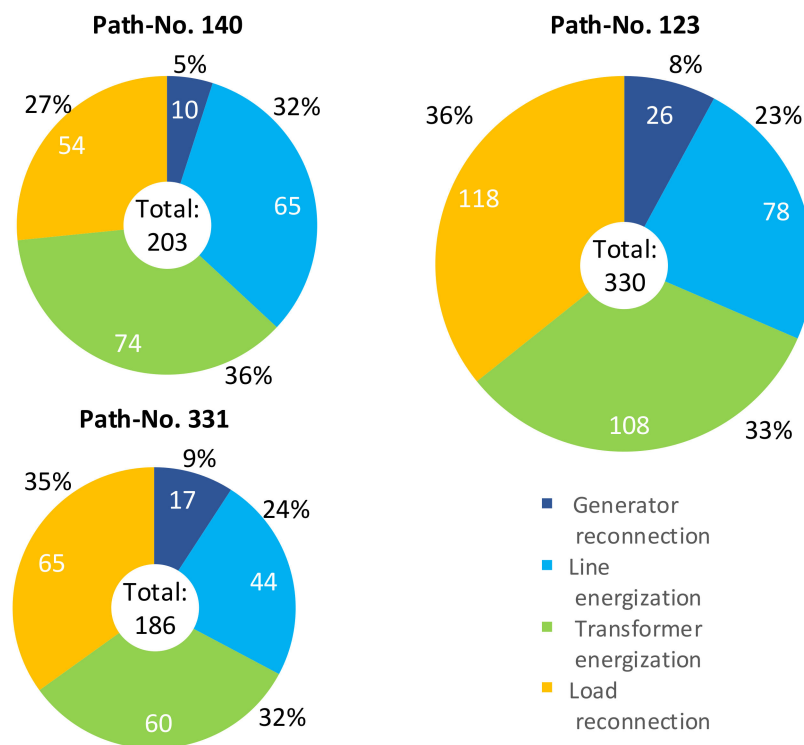

Figure 8. Share and total number of reconnected elements in Path-No. 140, Path-No. 123 and Path-No. 331 (Table S332)

Figure 9 presents the minimum and maximum dynamic and the static frequency observed on Path-No. 140 (Table S140) and Path-No. 331(Table S331) The maximum frequency limit is 51.5 Hz and the minimum frequency limit is 49 Hz. The system load step ability is more critical in the beginning of the restoration. Moreover, in the beginning of the restoration, the dynamic frequency deviation is higher than in the later phase. As depicted, the fastest simulated path—Path-No. 140—is close to the security limits but always above 49 Hz in comparison to the reference path.
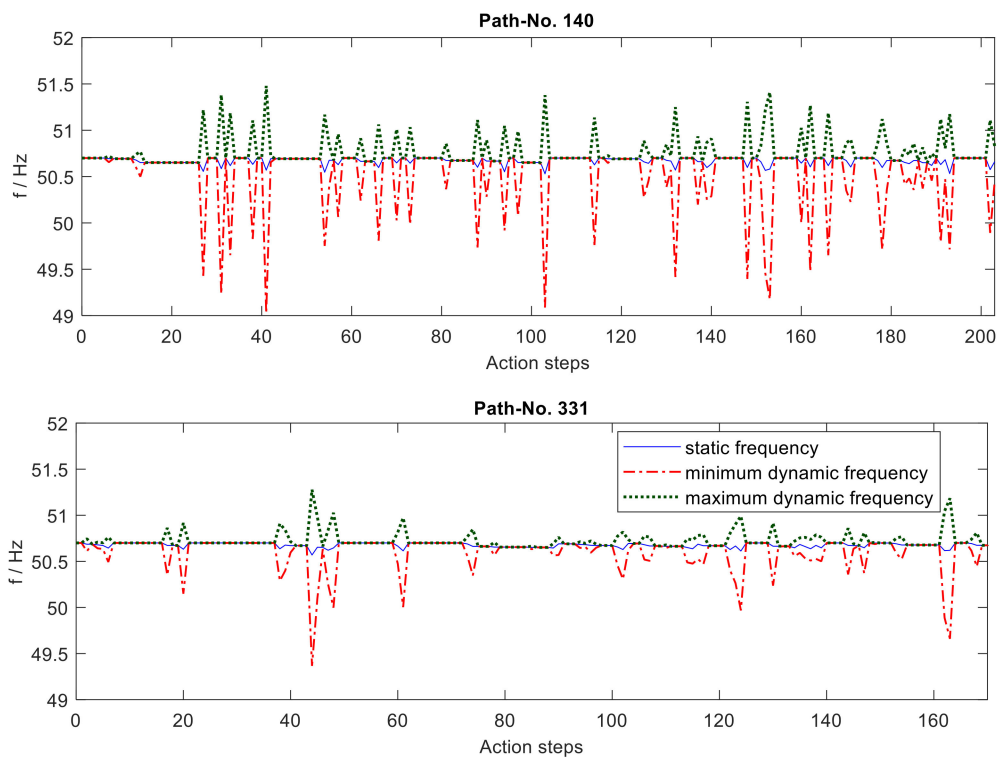
Figure 9. Dynamic and static frequency characteristic of Path-No. 140 and Path-No. 331 (Tables S140 and S331).

Figure 10 shows the maximum and minimum voltage observed on any of the 158 busses in the network after each action step in Path-No. 140. The voltage upper limit is 1.09 p.u. and the lower limit is 0.954 p.u. As depicted, it can be seen in the later action steps, the minimum voltage observed is close to but still above 0.954 p.u. This indicates that in the later stage of a system restoration, possible switching actions may be limited due to the defined voltage limits. This situation can be improved by reactive power management which is not modelled in the current automated algorithm described in this paper.
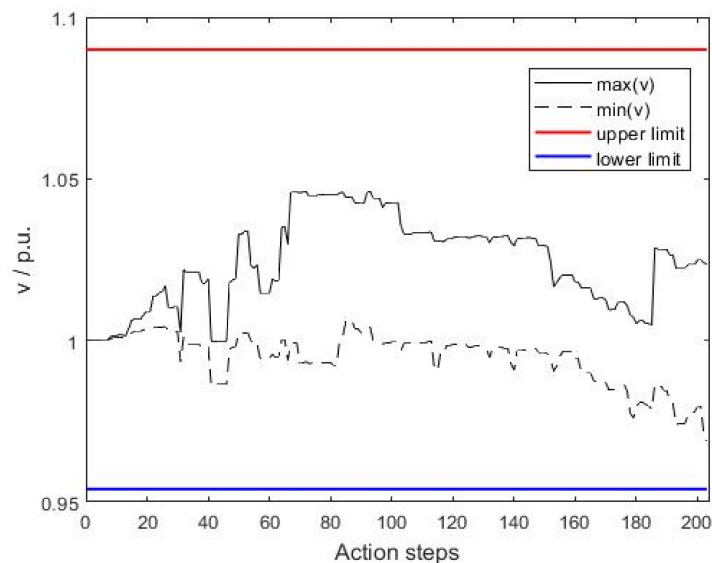
Figure 10. Voltage deviation of Path-No. 140 (Table S140).

Table 2 presents the comparison of the average load step during system restoration, the average use of the load step ability during the restoration period and the value of RES infeed reached in the last step of PSR.

As shown, Path-No. 140 has the highest value of the average load step during PSR, which means that a higher amount of load is re-connected in a lower number of carried-out switching actions. Besides, the loads which are chosen have larger values. The average use of the load step ability in the system during the restoration process is higher than the other paths.

Table 2. Evaluation of individual key performance indicators (KPI) and renewable energy sources (RES) infeed during the restoration process.

Path-No.	$\overline{\Delta P_{system}}$/MW	$\overline{\Delta P_{load\_step\_ability}}$	P_{RES}/MW
331 (reference)	5.79	0.18	59.66
140 (fastest)	6.98	0.46	42.51
123 (slowest)	3.17	0.13	72.85

7. Conclusions

The developed algorithm provides a framework to investigate a secure PSR within the given constraints. The constraints are adjusted according to the given parameters of the 110 kV and 20 kV network. The simulation results are acquired based on a customized Monte Carlo DFS and BFS. The developed algorithm and the extended approaches consider the dynamic behavior of the grid. Hence, it provides possible restoration paths for a pre-set percentage of the total system load. Parallelization of DFS and BFS algorithms on VSC allows a fast computation by conducting several MATLAB scripts on more than one processor, and the calculation of more states, and thus lays the basis for an investigation and optimization of the strategies. The evaluation of global and individual KPI of different paths provides a comparison of the system static and dynamic characteristics in different system restoration levels and will help in identifying suitable strategies. The presented algorithm improves the performance of the automated simulation of the restoration process and speeds up the calculation for investigating the restoration strategies. As discussed, the simulated Path-No. 140 is faster than the manually generated reference path according to the PSR concept of the Carinthia network, however, the dynamic frequency characteristics are close to critical limits.

Author Contributions: E.T.M. and Y.G.: methodology, software, validation, formal analysis, investigation, writing—original draft preparation, visualization; W.G.: conceptualization, writing—review and editing, funding acquisition; B.C., P.H. and M.Z.: software, writing—review and editing; W.W.: writing—review and editing; R.S.: resources, writing—review and editing; E.T. and L.F.: resources. All authors have read and agreed to the published version of the manuscript.

Conflicts of Interest: The authors declare no conflict of interest.

Nomenclature

$\overline{\Delta P_{system}}$	Average load step during system restoration
P_{FSR}	Increase of power demand
$\overline{\Delta P_{load\_step\_ability}[n]}$	Average use of load step ability in system
$\Delta P_{\max\_load}[n]$	Maximum load step ability of system
$\Delta P_{system\_load}[n]$	Power provided by the system where a load is re-connected
Δf_{int}	Integral of frequency deviation
$\Delta f_{max,dyn}$, $\Delta f_{min,dyn}$	Highest dynamic frequency deviation
$\Delta f_{max,stat}$	Highest static frequency deviation
Δv_{int}	Integral of voltage deviation
Δv_{max}	Highest voltage deviation
E_{FSR}	Energy provided during the entire power system restoration process
K_{CLPU}	Cold load pickup factor
K_{MAX}	Maximum value of CLPU factor
$N_{connected\_load}$	Number of switching action for re-connected loads
$N_{connected\_load}$	Number of steps, where loads are reconnected
P_{FSR}	Power provided during the power system restoration process
P_{RES}	Power of RES infeed
P_{state}	Steady state of load power
$P_{system,\, end}$	System power supply in level
P_{system}	Active power of load supplied by the total system
R_{0-N_R}	Starting points, which define roots of the tree
S_{l-j}	States, which define nodes in the tree
T_{CLPU}	Time for cold load pickup process
T_{FSR}	Restoration Time
f_0	Reference frequency
t_B	Time when the load is disconnected
t_H	Hold time
t_R	Reconnection time for cold load

References

1. Raoofsheibani, D.; Hinkel, P.; Ostermann, M.; Wellssow, W.H.; Nemati, M.; Neisius, H. Optimal restoration of distribution systems with active participation of volatile renewable generators. In Proceedings of the 2017 IEEE Manchester PowerTech, Manchester, UK, 18–22 June 2017; pp. 1–6.
2. Pham, T.T.H.; Besanger, Y.; Hadjsaid, N. New Challenges in Power System Restoration with Large Scale of Dispersed Generation Insertion. *IEEE Trans. Power Syst.* **2009**, *24*, 398–406. [CrossRef]
3. Buchholz, B.M.; Styczynski, Z.A. Integration of renewable and dispersed resources: Lessons learnt from German projects. In Proceedings of the 2006 IEEE Power Engineering Society General Meeting, Montreal, QC, Canada, 18–22 June 2006; p. 6.
4. Le, A.D.T.; Kashem, M.A.; Negnevitsky, M.; Ledwich, G. Control Strategy of Distributed Generation for Voltage Support in Distribution Systems. In Proceedings of the 2006 International Conference on Power Electronic, Drives and Energy Systems, New Delhi, India, 12–15 December 2006; pp. 1–6.
5. Delfino, B.; Denegri, G.B.; Invernizzi, M.; Morini, A.; Bonini, E.C.; Marconato, R.; Scarpellin, P. Black-start and restoration of a part of the Italian HV network: Modelling and simulation of a field test. *IEEE Trans. Power Syst.* **1996**, *11*, 1371–1379. [CrossRef]
6. Borghetti, A.; Migliavacca, G.; Nucci, C.A.; Spelta, S.; Tarsia, F. Simulation of the load following capability of a repowered plant during the first phase of the system restoration. In Proceedings of the IFAC Proceedings, Beijing, China, 5–9 July 1999; Volume 32, pp. 7231–7240.

7.   Agneholm, E. Cold Load Pick-up. Ph.D. Thesis, Department of Electric Power Engineering, Chalmers University of Technology, Goeteburg, Sweden, February 1999.

8.   Kumar, V.; Kumar H.C., R.; Gupta, I.; Gupta, H.O. DG Integrated Approach for Service Restoration under Cold Load Pickup. *IEEE Trans. Power Deliv.* **2010**, *25*, 398–406. [CrossRef]

9.   Adibi, M.M.; Fink, L.H. Power system restoration planning. *IEEE Trans. Power Syst.* **1994**, *9*, 22–28. [CrossRef]

10.   Adibi, M.M.; Kafka, R.J. Power system restoration issues. *IEEE Comput. Appl. Power* **1991**, *4*, 19–24. [CrossRef]

11.   Lindenmeyer, D.; Dommel, H.W.; Adibi, M.M. Power system restoration—A bibliographical survey. *Int. J. Electr. Power Energy Syst.* **2001**, *23*, 219–227. [CrossRef]

12.   Guo, Y.; Torabi-Makhsos, E.; Rossa-Weber, G.; Gawlik, W.; Schmaranz, R.; Hinkel, P.; Ostermann, M.; Wellssow, W.; Traxler, E. Review on Network Restoration Strategies as A Part of the RestoreGrid4RES Project. In Proceedings of the 15 Symposium Energieinnovation, Graz, Australia, 14–16 February 2018.

13.   Torabi, E.; Guo, Y.; Rossa-Weber, G.; Schrammel, M.; Gawlik, W.; Hinkel, P.; Zugck, M.; Raoofsheibani, D.W.W.; Schmaranz, R.; Traxler, E.; et al. Impact of renewable and distributed generation on grid restoration strategies. In Proceedings of the CIRED 2019-25th International Conference and Exhibition on Electricity Distribution, Madrid, Spain, 3–6 June 2019.

14.   Torabi, E.; Guo, Y.; Gawlik, W.; Hinkel, P.; Zugck, M.; Wellssow, W.; Schmaranz, R.; Traxler, E.; Fiedler, L. Parallel Breadth-and Depth-First Monte Carlo Tree Search Algorithms for Investigating Power System Restoration. In Proceedings of the 16 Symposium Energieinnovation, Graz, Australia, 12–14 February 2020.

15.   ENTSO-E. COMMISSION REGULATION (EU) 2017/2196 of 24 November 2017, Establishing a Network Code on Electricity Emergency and Restoration. Available online: https://www.entsoe.eu/network_codes/er/ (accessed on 28 February 2020).

16.   Browne, C.B.; Powley, E.; Whitehouse, D.; Lucas, S.M.; Cowling, P.I.; Rohlfshagen, P.; Tevener, S.; Perez, D.; Samothrakis, S.; Colton, S. A Survey of Monte Carlo Tree Search Methods. *IEEE Trans. Comput. Intell. AI Games* **2012**, *4*, 1–43. [CrossRef]

17.   Adibi, M.; Clelland, P.; Fink, L.; Happ, H.; Kafka, R.; Raine, J.; Scheurer, D.; Trefny, F. Power System Restoration—A Task Force Report. *IEEE Trans. Power Syst.* **1987**, *2*, 271–277. [CrossRef]

18.   Enacheanu, B.; Fontela, M.; Andrieu, C.; Pham, H.; Martin, A.; Gie-Idea, Y.B. New control strategies to prevent blackouts: Intentional islanding operation in distribution networks. In Proceedings of the CIRED 2005-18th International Conference and Exhibition on Electricity Distribution, Turin, Italy, 6–9 June 2005.

19.   Moser, M. Analyse und Bewertung von Netzwiederaufbau nach einer Versorgungsunterbrechung. Master's Thesis, Institute of Energy Systems and Electrical Drives, TU Wien, Vienna, Austria, 2019.

20.   Stadler, S.A. Cold Load Pickup. Master's Thesis, Institute of Electrical Power Systems, TU Graz, Graz, Austria, 2013.

21.   Ostermann, M.; Hinkel, P.; Raoofsheibani, D.; Wellssow, W.H.; Schneider, C. A minimum-regret-based optimization approach for power system restoration in EHV grids. In Proceedings of the 2017 IEEE Power & Energy Society General Meeting, Chicago, IL, USA, 16–20 July 2017; pp. 1–5.

22.   Collin, Z.; Dolev, S. Self-stabilizing depth-first search. *Inf. Process. Lett.* **1994**, *49*, 297–301. [CrossRef]

23.   Rao, V.N.; Kumar, V. Parallel depth first search. Part I. Implementation. *Int. J. Parallel Program.* **1987**, *16*, 479–499. [CrossRef]

24.   Niewiadomski, R.; Amaral, J.N.; Holte, R.C. A Parallel External-Memory Frontier Breadth-First Traversal Algorithm for Clusters of Workstations. In Proceedings of the 2006 IEEE International Conference on Parallel Processing, Columbus, OH, USA, 14–18 August 2006; pp. 531–538.